Nuclear-nuclear interaction mediated by a mechanically controlled nitrogen-vacancy-center spin in diamond

Wan-Jun Su,[1,2,*] Ya-Dong Wu,[2,†] Zhen-Biao Yang,[1] and Barry C. Sanders[2,3,4]

[1] *Fujian Key Laboratory of Quantum Information and Quantum Optics and Department of Physics, Fuzhou University,350116, China*

[2] *Institute for Quantum Science and Technology, University of Calgary, Alberta T2N 1N4, Canada*

[3] *Program in Quantum Information Science, Canadian Institute for Advanced Research,Toronto, Ontario M5G 1Z8, Canada*

[4] *Hefei National Laboratory for Physical Sciences at Microscale, University of Science and Technology of China, Hefei, Anhui 230026, China*

(Dated: May 28, 2019)

We propose a scheme to achieve nuclear-nuclear indirect interactions mediated by a mechanically driven nitrogen-vacancy (NV) center in diamond. Here we demonstrate two-qubit entangling gates and quantum-state transfer between two carbon nuclei in diamond. In such a system, the NV center interacts with a nearby nuclear spin via a dipole-dipole interaction. Under the quantum Zeno condition, the scheme is robust against decoherence caused by coupling between the NV center (nuclear spins) and the environment. Conveniently, precise control of dipole coupling is not required so this scheme is insensitive to fluctuating positions of the nuclear spins and the NV center. Our scheme provides a general blueprint for multi-nuclear-spin gates and for multi-party communication in a polygon geometry with each vertex occupied by a nuclear spin.

PACS numbers: 03.65.Xp,03.65.Vf,42.50.Dv,42.50.Pq

I. INTRODUCTION

Solid-state quantum systems are advantageous for quantum-information applications due to their inherent amenability to scaling [1]. Weakly coupled to the environment, nuclear spins have long coherence time in comparison with those of electron spins. Thus, nuclear spins are especially attrative for solid-state quantum storage [2] and for quantum gates [3]. Unfortunately, direct nuclear dipole-dipole interaction is negligible, which necessitates alternatives to couple nuclear spins. We propose using an extra auxiliary nitrogen-vacancy (NV) center electronic spin, which controls and mediates effective nuclear dipole-dipole indirect interaction.

NV center in diamond is a promising platform for highly sensitive nanoscale sensors [4, 5]. The NV center electronic spin has exceptional quantum properties including high sensitivity to external signals [6], and a long spin coherence time [7]. Additionally, NV center spin states can be prepared and read out by optical pulses or microwave pulses at room temperature [8]. These properties make NV center spin sensors an attractive candidate to detect nuclear-nuclear interactions [9–11], and open up a way to exploit its applications to solid-state quantum information. Recently, Chen et al. used periodical resets of an NV center to protect a nuclear quantum sensor against decoherence and relaxation of the NV center [12] .

Driving spin transitions of an NV center is the key to using NV center spins for nuclear-spin sensing. Except for optical and magnetic pluses, mechanical driving usually is applied to spin control. Significant progress in integrating NV centers with micro-electromechanical systems paves the way for spins coupled to mechanical resonators [13–16]. Using mechanical driving, MacQuarrie et al. demonstrated direct spin-phonon interactions at room temperature as a means to drive magnetically forbidden spin transitions [17].

However, for nuclear-nuclear indirect interaction, two crucial challenges remain to be addressed: (1) disorder in spin positioning and (2) small stress-coupling coefficient in driving spin transitions. Here we present an approach to overcome these challenges, to thereby achieve high-fidelity two-nuclear quantum gates and quantum-state transfer. In our scheme, an NV center is a mediator, coupling two nearby nuclear spins via dipole-dipole interactions. At the same time, mechanical (stress) wave is used to drive the magnetically forbidden spin transition $|m_s = -1\rangle \leftrightarrow |m_s = +1\rangle$ of the NV center. Our physical model requires that the driving-field Rabi frequency is sufficiently weak relative to the dipole-coupling strength. In experiments, normally, the stress-coupling coefficient is small so that large stress is required to produce a driving field [17]. However, the small stress-coupling coefficient is helpful for our scheme, and large stress is not required.

Driving the NV center is analogous to frequent measurements in the quantum Zeno effect [18]. Under the quantum Zeno condition [19], coherent evolution between nuclear spins is achieved within the quantum Zeno dark subspaces with eigenvalue zero. Our approach has the following advantages: (1) time evolution within the quantum Zeno dark subspaces decouples the NV center and nuclear spins from the environment and (2) desired conditional manipulations do not require precise control of

*Electronic address: wanjunsu@fzu.edu.cn

†Electronic address: yadong.wu@ucalgary.ca

the dipole coupling. Hence, our scheme is robust against variations and uncertainties in the positions of the NV center and nuclear spins.

Paper is organized as follows. Section II describes the relevant background of our scheme, such as the quantum Zeno effect, the dipole-dipole interaction and mechanical driving on the NV center spin. Section III and Section IV presents our physical model and the quantum dynamics of the model. We propose a scheme to achieve entangling gates and quantum-state transfer based on this dynamics. We investigate fidelities versus parameter fluctuations (scaled Rabi frequency, dipole-dipole coupling strength, etc.) via numerical simulations. Section V presents the discussions of our physical model at ambient conditions and further applications. Section VI is our conclusion.

II. BACKGROUND

In this section, we present the relevant background of our scheme. First, we describe the quantum Zeno effect and quantum Zeno dynamics. Second, we present the relevant background of dipole-dipole interaction and magnetic-dipolar coupling in an electron-nuclear spin system. Third, we describe mechanical spin control of an NV center in diamond, which offers a route to quantum spin control of magnetically forbidden transitions.

A. Quantum Zeno effect

The quantum Zeno effect occurs, when frequent measurements are performed on a quantum system [19]. Repeated projective measurements block evolution of the quantum system prepared in a non-degenerate eigenstate of the measurement observable, so that the system is frozen in its initial state, which protects the system from decohering [20].

Frequent measurements cause wave-function collapse, and the system is reduced to an undecayed state. If measurement time is short enough, the probability of decay grows quadratically with the measurement time [19]. Consider taking N measurements, separated by time T/N. The probability that the state survives for time T goes to one in the limit $N \to \infty$. Hence, a continuously observed state never decays.

Quantum Zeno dynamics is achieved by employing strong continuous coupling, replacing projective measurements, which yield the "undecayed" result and hinder evolution of the quantum system [21, 22]. By continuous coupling, the system evolves away from its initial state and is forced to evolve in a set of orthogonal subspaces (quantum Zeno subspaces) of the Hilbert space. A dynamical superselection rule arises in the strong coupling limit.

Short timescales can be physically associated with strong couplings. Dynamical evolution of the quantum system is governed by the Hamiltonian [21]

$$H_K = H + KH_c, \tag{1}$$

where K is the coupling constant, H is the Hamiltonian of the quantum system to be studied, and H_c is an additional interaction Hamiltonian performing the continuous coupling.

The time evolution operator is

$$U_K(t) = \exp(-iH_K t). \tag{2}$$

In the limit $K \to \infty$ ("infinitely strong measurement" or "infinitely quick detector"), the time evolution operator $U_K(t)$ is dominated by $\exp(-iKH_c t)$. Consider P_n the eigenprojection of H_c, corresponding to the eigenvalue λ_n; i.e.,

$$H_c = \sum_n \lambda_n P_n. \tag{3}$$

Note that in Eq. (3), $\lambda_n \neq \lambda_m$ for $n \neq m$.

In the limit $K \to \infty$, an effective superselection rule arises, and the Hilbert space is split into a set of quantum Zeno subspaces. The subspaces decouple from each other so they are invariant under the evolution. The system, with respect to H, is dominated by the evolution operator [21]

$$U_Z(t) = \lim_{K\to\infty} \exp(iKH_c t)U_K(t), \tag{4}$$

which can be shown to have the form

$$U_Z(t) = \exp(iH_Z t), \tag{5}$$

where

$$H_Z = \sum_n P_n H P_n, \tag{6}$$

is the Zeno Hamiltonian.

Thus, the limiting time evolution operator $U_K(t)$ in Eq. (2) can be rewritten as

$$\begin{aligned} U_K(t) &\sim \exp(-iKH_c t)U_Z(t) \\ &= \exp\left[-i\sum_n (K\lambda_n P_n + P_n H P_n)t\right], \end{aligned} \tag{7}$$

whose block-diagonal structure is explicit and yields the Zeno subspaces. When quantum Zeno dynamics takes effect, strong continuous coupling destroys interference between different Zeno subspaces.

The quantum Zeno effect has been experimentally verified in trapped ions [23] and cavity quantum electrodynamics (CQED) [24–26]. Recently, quantum controls using quantum Zeno effect have been realized in circuit-QED systems [27] and NV center systems [28]. Gourgy et al. demonstrated that the quantum Zeno effect can be used to detect an escape from the system eigenstate, serving as a built-in form of error detection [27]. A nitrogen nuclear spin acts as a three-level quantum switch, while an NV center electron spin acts as a two-level register [28]. Taking advantage of the quantum Zeno effect, the system can remain in the Zeno subspace due to the frequent projection by the environment.

B. Dipole-dipole interactions

Dipole-dipole interaction, the key element underlying our proposal is a phenomenon discussed in the context of Rydberg atoms [29]. Rydberg atoms with principal quantum number $n \gg 1$ have exaggerated atomic properties including dipole-dipole interactions that scale as n^4 and radiative lifetimes that scale as n^3. Suppose r is the separation between two particles; the interaction of ground-state atoms is dominated by $1/r^6$ van der Waals forces at short range and $1/r^3$ magnetic dipole-dipole forces beyond about 30 nm [29]. When spacings exceed 1μ m, the interaction is weak and less than 1 Hz in frequency units, which implies that an array of neutral atom qubits can be structurally stable. The dipole-dipole interaction is extremely sensitive to small low-frequency electric fields. Using such fields, strength and angular dependence of Rydberg-Rydberg interactions are tunable [30].

Dipole-dipole interactions enable the capabilities for future applications in quantum information processing [29, 30]. Numerous proposals suggest dipole-dipole interactions to implement quantum logic gates [31–33] and to prepare quantum states in different quantum systems, such as CQED [34, 35] and NV centers in diamond [36]. Recently, Wu et al. proposed a promising scheme to realize Rydberg-interaction two-qubit gates, which relies on adiabatic passage and phase control of driving fields [37].

Magnetic dipole-dipole interactions usually take place in dipolar spin systems [38–41], such as solid-state spin ensembles [38], hybrid systems [39], and NV-P1 coupling systems [40] (P1 is substitutional-nitrogen electronic spins). The Hamiltonian describing a nuclear spin coupled to an NV center via the magnetic dipolar coupling is [41]

$$H_{\rm DD} = g\left[\hat{\boldsymbol{S}}\cdot\hat{\boldsymbol{I}} - 3(\hat{\boldsymbol{S}}\cdot\boldsymbol{r})(\hat{\boldsymbol{I}}\cdot\boldsymbol{r})\right], \tag{8}$$

where $\hat{\boldsymbol{S}}$ and $\hat{\boldsymbol{I}}$ are the spin operators of the NV and the nuclear spin respectively, and $g = (\mu_0\gamma_{\rm e}\gamma_{\rm N})/(4\pi r^3)$ with μ_0 the magnetic permeability, $\gamma_{\rm e}$ and $\gamma_{\rm N}$ the gyromagnetic ratio of the electron spin and nuclear spin, respectively. Here r is the distance between the NV center and nuclear spin, and $\boldsymbol{r}$ is the unit vector connecting them. The last term defines the angular dependence of the coupling between the NV center and nuclear spin.

During the dipolar coupling, the NV electron spin feels a magnetic field $B_{\rm DD}$ caused by nuclear spin and vice versa. The effect of $B_{\rm DD}$ is closely related to relative orientations of spins. Denote θ as the angle between $\boldsymbol{r}$ and $\mathbf{z}$, where $\mathbf{z}$ axis is the [111] crystal axis. By choosing $\theta = 54.7°$ (also known as the "magic angle"), $B_{\rm DD}$ is perpendicular to $\mathbf{z}$ [41]. Then, the two-spin states $|m_s^{NV}, m_s^N\rangle = \{|0,+1/2\rangle, |-1,-1/2\rangle\}$ are strongly mixed by the dipolar fields at the resonance condition. The dipole-coupling process dominates interactions between the NV spin and nuclear spins. In this case, in energy, the state $|m_s=+1\rangle_{\rm NV}$ is far from $|m_s=0\rangle_{\rm NV}$ and $|m_s=-1\rangle_{\rm NV}$ states, therefore, has a negligible effect on the dipole coupling.

An optical illumination polarizes the NV center spin $|m_s=-1\rangle_{\rm NV}$ into $|m_s=0\rangle_{\rm NV}$, whereas the component of $B_{\rm DD}$ leads to flip-flops between the NV center and nuclear spin determined by Eq. (8). Dipole coupling NV-^{13}C or NV-^{14}N have been experimentally achieved at room temperature [42–44]. At room temperature, the hyperfine coupling between the ^{14}NV electronic spin and ^{13}C nuclear spin has been achieved with the coupling parameters of $g \sim 2\pi \times 2.0$ MHz [45]. Dipole-dipole interactions can also be used to manipulate multiple nuclear spins. Recently, Cramer et al. demonstrated quantum error correction by encoding a logical qubit in three nuclear spins mediated by an ancillary NV center [46].

C. Mechanically-driven NV center spin

Driving spin transitions is the key to using NV center spins for bio-sensing or for quantum information processing [13–16]. Magnetic fields or optical pulses usually are applied to control spin. Resonant lattice vibrations provide another avenue to manipulate NV center electronic spins. Spin-phonon interactions could offer a way to achieving quantum spin control of magnetically forbidden transitions.

By aligning a static magnetic field, a single NV center can be isolated from other NV centers in a diamond [17]. The diamond substrate acts as an acoustic Fabry-Perot cavity. A high-overtone bulk acoustic resonator(HBAR) is put onto one face of the diamond [16, 17]. Applying a voltage across the HBAR launches a stress wave into the diamond.

The Hamiltonian describing an NV center coupled via stress through its ground-state spin is [17]

$$H_{\rm drive} = \epsilon_\parallel\sigma_\parallel\hat{S}_z^2 - \epsilon_\perp\sigma_x(\hat{S}_x^2 - \hat{S}_y^2) + \epsilon_\perp\sigma_y(\hat{S}_x\hat{S}_y + \hat{S}_y\hat{S}_x), \tag{9}$$

where $\epsilon_\parallel$ and $\epsilon_\perp = 0.03$ MHz/Mpa are axial and perpendicular stress-coupling constants, and $\hat{S}_x$, $\hat{S}_y$, $\hat{S}_z$ are x, y and z components of the spin-1 operator, respectively. The axial stress $\sigma_\parallel$ shifts $|m_s=-1\rangle_{\rm NV}$ and $|m_s=+1\rangle_{\rm NV}$ equivalently and, therefore, has no effect on mechanical spin control performed on the $|m_s=\pm1\rangle_{\rm NV}$ spin. However, perpendicular stress couples $|m_s=-1\rangle_{\rm NV}$ and $|m_s=+1\rangle_{\rm NV}$, allowing a direct $|m_s=-1\rangle_{\rm NV} \leftrightarrow |m_s=+1\rangle_{\rm NV}$ spin transition to be driven by a stress wave. In the $\hat{S}_z$ basis, this transition is magnetically forbidden by the magnetic dipole selection rule

During the mechanical driving of the NV center, choosing a HBAR with $\omega_{\rm HBAR} = 2\pi \times 1.076$ GHz, a stress wave is launched into the diamond with the corresponding perpendicular stress $\sigma_\perp \approx 7$ Mpa. Therefore, a spin driving field with Rabi frequency $\Omega \sim 2\pi \times 210$ kHz is achieved [17].

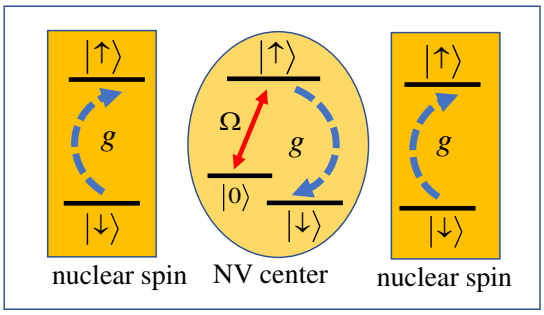

FIG. 1: (Color online) Illustration of the basic principle of indirect interaction between two nuclear spins mediated by a NV center. The interaction between the NV center and nuclear spins occurs via coupling dipoles on the transition $|\uparrow\rangle \leftrightarrow |\downarrow\rangle$, with coupling strength g. The transition $|0\rangle \leftrightarrow |\uparrow\rangle$ of the NV center is resonantly driven by mechanical (stress) wave of Rabi frequency Ω.

III. PHYSICAL MODEL

In this section, we first describe a system comprising a NV center coupled to two nuclear spins. Then we propose a physical model of the NV-nuclear system, similar to frequent measurements in quantum Zeno effect. Finally, we describe the master equation for our model.

Our goal is to use the NV center as a mediator for indirect coherent interactions between two nuclear spins in diamond. The schematic setup is shown in Fig. 1. A NV center in diamond mediates two distinguishable nuclear spins. The ground state of the NV center is a spin-1 triplet state, labeled ^3A, with zero-field splitting $D = 2.87$ GHz between the $|m_s = 0\rangle$ and $|m_s = \pm 1\rangle$ states. By applying an external magnetic field along the NV center symmetry axis, one can lift the degeneracy of $|m_s = -1\rangle$ and $|m_s = +1\rangle$ [47].

For simplicity, we denote the following states: NV center spin states

$$\begin{aligned} |\downarrow\rangle_{\rm NV} &:= |m_s = 0\rangle\,, \\ |\uparrow\rangle_{\rm NV} &:= |m_s = -1\rangle\,, \\ |0\rangle_{\rm NV} &:= |m_s = +1\rangle\,, \end{aligned} \tag{10}$$

and nuclear spin states

$$\begin{aligned} |\downarrow_i\rangle &:= \left|m_s = -\frac{1}{2}, m_I = 0\right\rangle, \\ |\uparrow_i\rangle &:= \left|m_s = +\frac{1}{2}, m_I = 0\right\rangle, \end{aligned} \tag{11}$$

where i denotes the nuclear spin. We assume that the interaction between the NV center and nuclear spins only occurs via dipole coupling on selected transitions $|\uparrow\rangle \leftrightarrow |\downarrow\rangle$, whereas dipoles on other transitions do not interact with nuclear spins due to different frequencies or polarizations [40]. When the energy between $|\uparrow\rangle_{\rm NV}$ and $|\downarrow\rangle_{\rm NV}$ of the NV center matches the transition frequency of the nuclear spin, the flip-flop process is most efficient. A perpendicular stress couples $|0\rangle_{\rm NV}$ and $|\uparrow\rangle_{\rm NV}$ of the NV center, allowing a direct spin transition $|0\rangle_{\rm NV} \leftrightarrow |\uparrow\rangle_{\rm NV}$ to be resonantly driven by a gigahertz-frequency mechanical (stress) wave.

Under the rotating-wave approximation, the system can be described by the following effective Hamiltonian in the interaction picture: ($\hbar = 1$)

$$\begin{aligned} H =& H_{\rm drive} + H_{\rm DD}, \\ H_{\rm drive} =& \Omega\ |0\rangle_{\rm NV}\langle\uparrow| + {\rm H.c.}, \\ H_{\rm DD} =& \sum_{i=1,2} g_i\, \sigma^{\rm NV}_{\downarrow\uparrow}\sigma^{i}_{\uparrow\downarrow} + {\rm H.c.}, \end{aligned} \tag{12}$$

where $H_{\rm drive}$ describes the stress waves driving the NV center, and $H_{\rm DD}$ describes the dipole-dipole interaction. Ω is the Rabi frequency relevant to the driving field, $\sigma_{\alpha\beta} = |\alpha\rangle\langle\beta|$ are dipole operators and $\alpha, \beta \in \{\downarrow, \uparrow\}$. g_i is the coupling constant between interacting dipoles related to the separation between the NV center spin and nuclear spins.

In our scheme, dipole-dipole interactions between the NV center and nuclear spins are taken as an additional interaction Hamiltonian, being an analog of the strong continuous coupling in quantum Zeno dynamics. The Hamiltonian in Eq. (1) can be rewritten as

$$H_K = H_{\rm drive} + H_{\rm DD}, \tag{13}$$

where $K = g/\Omega$ describes the ratio of the dipole-coupling strength and the driving- field Rabi frequency.

We choose the dipole-coupling strength $g \sim 2\pi \times 2$ MHz, corresponding to the magnetic dipole-dipole interaction between ^{14}NV electronic spin and ^{13}C nuclear spin [45], and the spin driving-field Rabi frequency $\Omega \sim 2\pi \times 210$ kHz [17]. The driving-field Rabi frequency is sufficiently weak relative to the dipole-coupling strength, which satisfies the quantum Zeno condition $K \to \infty$. Then time evolution of quantum state inside each subspace is independent from each other. Here we call the eigenspace with eigenvalue zero the quantum Zeno dark subspace. If the initial state is within the quantum Zeno dark subspace, effective system Hamiltonian is equal to the Zeno Hamiltonian in Eq. (6), and time evolution of our system can be simplified to

$$U(t) \sim \exp\left[-i\sum_n \left(P_n H_{\rm drive} P_n\right) t\right]. \tag{14}$$

Here, P_n are the eigenprojections of $H_{\rm DD}$. In this case, quantum state evolves within the dark subspace, which is a decoherence-free subspace.

To model the system's dynamics, decoherence effects, such as the spontaneous decay of the NV center and nuclear spin, are taken into account. We employ Lindblad formalism to the following master equation [48]

$$\frac{\partial\rho}{\partial t} = -i[\rho, H] + \gamma_{\rm NV} L_{\rm NV}[\rho] + \gamma_{\rm N} L_{\rm N}[\rho], \tag{15}$$

where $\gamma_{\rm NV}$ is the relaxation rate of NV spins, $\gamma_{\rm N}$ is the relaxation rate of nuclear spin, and the general form

$$L[\rho]=\sigma\rho\sigma^{+}-\frac{1}{2}\left(\sigma^{+}\sigma\rho-\rho\sigma^{+}\sigma\right), \tag{16}$$

corresponds to the relaxation of electron spins or nuclear spins. Here, σ is the dipole operator as $\sigma_{\alpha\beta}$.

During the system dynamics, the system is initially in the state $|\Psi_0\rangle$, and then evolves under Eq. (12) for a choosing time, resulting in a final density ρ. The fidelity is defined as [49]

$$F:=\langle\Psi_0|\,\rho\,|\Psi_0\rangle\,, \tag{17}$$

where $\rho=|\Psi_t\rangle\langle\Psi_t|$. In the following, we show how to achieve the quantum entangling gates and quantum state transfer based on this model.

IV. QUANTUM DYNAMICS AND QUANTUM INFORMATION PROCESSING

In this section, we first describe time evolution of the system states based on the model above. Second, we show an implementation scheme to achieve two-qubit entangling gates. Third, based on the same dynamics, we show how to carry out quantum-state transfer. We also numerically discuss the factors affecting the fidelity.

A. Quantum dynamics

We assume that quantum information is encoded in nuclear spin states $|\uparrow\rangle$ and $|\downarrow\rangle$, and the NV center electron spin is an ancillary system, which is initially prepared in $|0\rangle$ state. For simplicity, we suppose there is only single excitation during the whole system's evolution [50].

Considering an initial system state $|\uparrow_1\rangle|\uparrow_2\rangle|0\rangle_{\rm NV}$, no dipole-dipole interaction takes effect. Time evolution of the system is within the subspace $\{\ |\uparrow_1\rangle|\uparrow_2\rangle|0\rangle_{\rm NV}, |\uparrow_1\rangle|\uparrow_2\rangle|\uparrow\rangle_{\rm NV}\ \}$. The driving field only causes a single-qubit rotation. After a single Rabi cycle, the nuclear spin state returns to its original state timing a π phase shift.

$$|\uparrow_1\rangle|\uparrow_2\rangle\rightarrow e^{i\Omega t}|\uparrow_1\rangle|\uparrow_2\rangle\rightarrow-|\uparrow_1\rangle|\uparrow_2\rangle\,. \tag{18}$$

When we consider an initial system state $|\uparrow_1\rangle|\downarrow_2\rangle|0\rangle_{\rm NV}$, the whole system evolves in a single-excitation subspace S_1 spanned by

$$\begin{aligned}
|\phi_1\rangle&=|\uparrow_1\rangle|\downarrow_2\rangle|0\rangle_{\rm NV}\,,\\
|\phi_2\rangle&=|\uparrow_1\rangle|\downarrow_2\rangle|\uparrow\rangle_{\rm NV}\,,\\
|\phi_3\rangle&=|\uparrow_1\rangle|\uparrow_2\rangle|\downarrow\rangle_{\rm NV}\,,\\
|\phi_4\rangle&=|\downarrow_1\rangle|\uparrow_2\rangle|\uparrow\rangle_{\rm NV}\,,\\
|\phi_5\rangle&=|\downarrow_1\rangle|\uparrow_2\rangle|0\rangle_{\rm NV}\,.
\end{aligned} \tag{19}$$

Therefore, in the subspace S_1, setting $g_i=g$ to be constant coupling coefficients, the interaction Hamiltonian in Eq. (12) is simplified as

$$\begin{aligned}
H_{\rm drive}&=\Omega(|\phi_1\rangle\langle\phi_2|+|\phi_4\rangle\langle\phi_5|)+{\rm H.\,c.},\\
H_{\rm DD}&=g(|\phi_2\rangle+|\phi_4\rangle)\langle\phi_3|+{\rm H.\,c.}\,.
\end{aligned} \tag{20}$$

Then, under the Zeno condition $\Omega\ll g$, the whole Hilbert subspace is split into three invariant Zeno subspaces according to the degeneracy of eigenvalues of $H_{\rm DD}$,

$$\begin{aligned}
Z_0&=\{|\phi_1\rangle\,,|\psi_1\rangle\,,|\phi_5\rangle\},\\
Z_+&=\{|\Psi_+\rangle\},\\
Z_-&=\{|\Psi_-\rangle\},
\end{aligned} \tag{21}$$

with three corresponding eigenvalues $\lambda_1=0$, $\lambda_2=\sqrt{2}g$, $\lambda_3=-\sqrt{2}g$, and where

$$\begin{aligned}
|\psi_1\rangle&=\frac{1}{\sqrt{2}}(-|\phi_2\rangle+|\phi_4\rangle),\\
|\Psi_+\rangle&=\frac{1}{2}(|\phi_2\rangle+\sqrt{2}\,|\phi_3\rangle+|\phi_4\rangle),\\
|\Psi_-\rangle&=\frac{1}{2}(|\phi_2\rangle-\sqrt{2}\,|\Phi_3\rangle+|\phi_4\rangle).
\end{aligned} \tag{22}$$

Within the quantum Zeno dark supspace Z_0, the effective Hamiltonian is given by

$$H_{\rm eff}=\frac{\Omega}{\sqrt{2}}(-|\phi_1\rangle+|\phi_5\rangle)\langle\psi_1|+{\rm H.\,c.}\,. \tag{23}$$

The general evolution of Eq. (23) by solving the Schrödinger equation with the interaction time t is

$$\begin{aligned}
|\Psi_{(t)}\rangle=&\frac{1}{2}\Big[(1+\cos\Omega t)\,|\phi_1\rangle+(1-\cos\Omega t)\,|\phi_5\rangle\\
&+\sqrt{2}i\sin\Omega t\,|\psi_1\rangle\Big].
\end{aligned} \tag{24}$$

By choosing interaction time $t=\pi/\Omega$, the final state becomes $|\Psi_{(t)}\rangle=|\downarrow_1\rangle|\uparrow_2\rangle|0\rangle_{\rm NV}$. Due to the symmetry of this system, an initial state of the system $|\downarrow_1\rangle|\uparrow_2\rangle|0\rangle_{\rm NV}$, after a time $t=\pi/\Omega$, evolves to $|\uparrow_1\rangle|\downarrow_2\rangle|0\rangle_{\rm NV}$.

Similar to the step above, when the system is in initial state $|\downarrow_1\rangle|\downarrow_2\rangle|0\rangle_{\rm NV}$, the whole system evolves in a single-excitation subspace S_2 spanned by:

$$\begin{aligned}
|\phi_6\rangle&=|\downarrow_1\rangle|\downarrow_2\rangle|0\rangle_{\rm NV}\,,\\
|\phi_7\rangle&=|\downarrow_1\rangle|\downarrow_2\rangle|\uparrow\rangle_{\rm NV}\,,\\
|\phi_8\rangle&=|\downarrow_1\rangle|\uparrow_2\rangle|\downarrow\rangle_{\rm NV}\,,\\
|\phi_9\rangle&=|\uparrow_1\rangle|\downarrow_2\rangle|\downarrow\rangle_{\rm NV}\,.
\end{aligned} \tag{25}$$

Therefore, under the quantum Zeno condition, the invariant Zeno subspaces S_2 are

$$\begin{aligned}
Z_0&=\{|\phi_6\rangle\,,|\psi_2\rangle\},\\
Z_+&=\{|\Psi_+\rangle\},\\
Z_-&=\{|\Psi_-\rangle\},
\end{aligned} \tag{26}$$

the corresponding eigenvalues $\lambda_1 = 0$, $\lambda_2 = \sqrt{2}g$, $\lambda_3 = -\sqrt{2}g$, where

$$
\begin{aligned}
|\psi_2\rangle &= \frac{1}{\sqrt{2}}(-|\phi_8\rangle + |\phi_9\rangle), \\
|\Psi_+\rangle &= \frac{1}{2}(\sqrt{2}|\phi_7\rangle + |\phi_8\rangle + |\phi_9\rangle), \\
|\Psi_-\rangle &= \frac{1}{2}(-\sqrt{2}|\phi_7\rangle + |\phi_8\rangle + |\phi_9\rangle).
\end{aligned} \tag{27}
$$

Because the initial state $|\phi_6\rangle$ is orthogonal to $|\psi_2\rangle$, $|\Psi_+\rangle$ and $|\Psi_-\rangle$, effective Hamiltonian $H_{eff} = 0$. The state $|\downarrow_1\rangle|\downarrow_2\rangle|0\rangle_{\rm NV}$ remains unchanged during system evolution.

B. Quantum entangling gate

Recently, Leonardo et al. proposed a scheme to realize nonperturbative entangling gates between distant qubits using uniform cold atom chains [51]. In their work, an ideal mirror inverting dynamics generates a quantum gate G between qubit A and qubit B, which reads

$$
G|a\rangle|b\rangle = e^{i\phi_{ab}}|b\rangle|a\rangle, \tag{28}
$$

where $a, b \in \{\downarrow, \uparrow\}$ in the computational basis. Based on time evolution of our physics model, we can achieve the entangling gate of two distant nuclear spins in diamond. For a duration of $T = \pi/\Omega$, the logical states of nuclear spins become

$$
\begin{aligned}
&|\uparrow_1\rangle|\uparrow_2\rangle \rightarrow -|\uparrow_1\rangle|\uparrow_2\rangle, \\
&|\uparrow_1\rangle|\downarrow_2\rangle \rightarrow |\downarrow_1\rangle|\uparrow_2\rangle, \\
&|\downarrow_1\rangle|\uparrow_2\rangle \rightarrow |\uparrow_1\rangle|\downarrow_2\rangle, \\
&|\downarrow_1\rangle|\downarrow_2\rangle \rightarrow |\downarrow_1\rangle|\downarrow_2\rangle,
\end{aligned} \tag{29}
$$

which corresponds to a two-qubit entangling gate between the distant nuclear spins. The ancillary system (NV center), initially prepared in $|0\rangle$ state, is entangled with the logical qubits during the gate operation, becoming once again disentangled by the end of the operation.

To verify the analytical results, we use numerical simulations to find the influences of the interaction. Our model is valid when $\Omega \ll g$. Thus, we should consider the influence of the ratio Ω/g on the fidelity of the entangling gate. Fig. 2 presents the fidelity as a function of Ω/g disregarding the decay. Not surprisingly, the fidelity decreases as the ratio Ω/g increases. The fidelity is 0.98, even when $\Omega/g = 0.15$. However, the interaction period $T = \pi/\Omega$ depends on Ω, then a smaller ratio Ω/g results in longer operating time and increased decoherence. To balance the fidelity and the operating time, we choose $g \sim 2\pi \times 2$ MHz and $\Omega \sim 2\pi \times 210$ kHz to satisfy $\Omega/g = 0.1$ in the following discussions.

The manipulation time depends on the stress-wave Rabi frequency. In our model, the NV center resonantly interacts with the driving field of frequency $\omega_{\rm drive}$, and

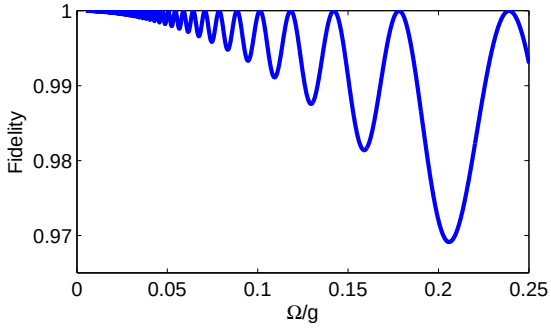

FIG. 2: (Color online) The influence of the ratio Ω/g on the fidelity of the two-qubit entangling gate under ideal conditions. $\Omega/g \in [0.005, 0.25]$ and $\gamma_{\rm N} = \gamma_{\rm NV} = 0$.

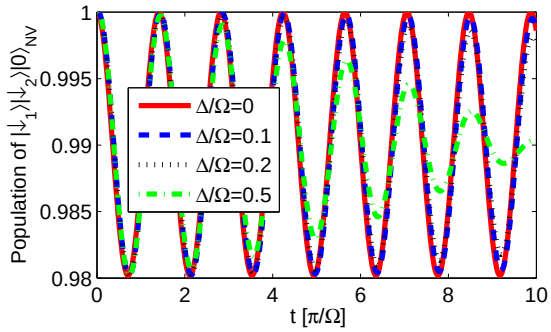

FIG. 3: (Color online) The population of $|\downarrow_1\rangle|\downarrow_2\rangle|0\rangle_{\rm NV}$ as a function of the scaled time, considering the influence of detuning. The scaled ratio Δ/Ω ranges from 0 to 0.5, $\gamma_{\rm N} = \gamma_{\rm NV} = 0$, with $g \sim 2\pi \times 2$ MHz and $\Omega \sim 2\pi \times 210$ kHz.

the corresponding transition energy of $|0\rangle \leftrightarrow |\uparrow\rangle$ is $\hbar\omega_{\uparrow 0}$. However, under ambient conditions, the quantum dynamics is affected by the off-resonant coupling, which will cause errors (phase shifts). We add fluctuating term in the driving field, so $H_{\rm drive}$ can be rewritten as

$$
H_{\rm drive} = \Omega \cdot e^{-i\Delta t}|0\rangle_{\rm NV}\langle\uparrow| + \text{H. c.}, \tag{30}
$$

where $\Delta := \omega_{\uparrow 0} - \omega_{\rm drive}$ describes the off-resonant coupling. The population of state $|\downarrow_1\rangle|\downarrow_2\rangle|0\rangle_{\rm NV}$, as a function of the interaction time and scaled off-resonant coupling Δ/Ω, is shown in Fig. 3. When the requirement $\Delta/\Omega < 0.2$ is met, small fluctuations of the population occur. Considering a small deviation of the resonant interaction between the driving field and NV center, we find that the average gate fidelity equals 0.995 with $\Delta/\Omega = 0.1$. The entangling gate is robust against fluctuations of the driving field, which is important to suppress errors.

The analysis above disregards the effects of decay. We now analyze how the gate operation is affected by desired dissipation according to Eq. (15). Assuming scaled spontaneous decay rates $\gamma_{\rm NV}/g = \gamma_{\rm N}/g = 0.001$, Fig. 4(a) displays the dynamics of populations of nuclear spins states as a time function. At the end of interaction time T, $\rho_{\uparrow_1\uparrow_2}$ and $\rho_{\downarrow_1\uparrow_2}$ are about 0.985. As shown in Fig. 4(b), the fi-

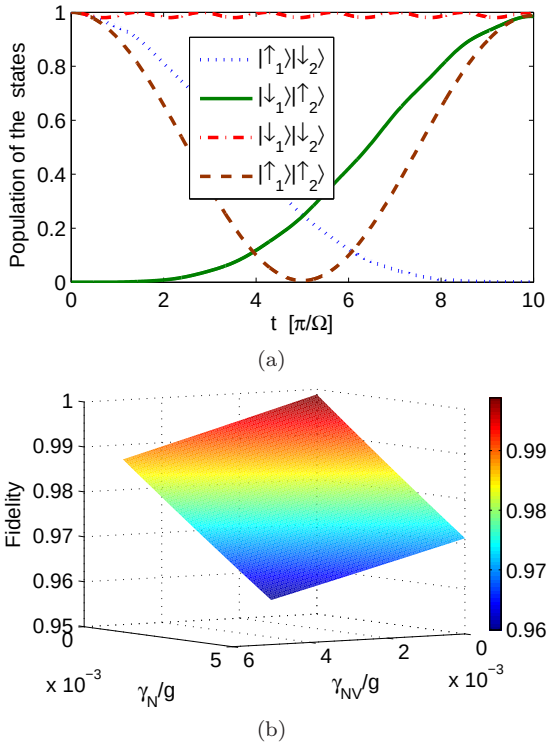

FIG. 4: (Color online) The influence of decoherence on realization of the two-qubit entangling gate, for $g \sim 2\pi \times 2$ MHz and $\Omega \sim 2\pi \times 210$ kHz. (a) Dynamical evolution of the populations during the gate operation, with $\gamma_{\rm NV}/g = \gamma_{\rm N}/g = 0.001$. (b) The fidelity of the entangling gate versus $\gamma_{\rm NV}/g$ and $\gamma_{\rm N}/g$.

delity remains high (> 0.96) with small scaled decay rates $\gamma_{\rm NV}/g$ and $\gamma_{\rm N}/g$, implying that the driving decouples the NV spin from the unwanted influence of environment.

C. Quantum-state transfer

Reliable quantum-state transfer (QST) between distant qubits has become a significant goal of quantum physics research, owing to its potential application in a scalable quantum information processing [52–54]. If the system is initially in the state

$$|\Psi_0\rangle = (\alpha\,|\downarrow_1\rangle + \beta\,|\uparrow_1\rangle)\,|\downarrow_2\rangle\,|0\rangle_{\rm NV}\,, \tag{31}$$

where $\alpha,\ \beta \in \mathbb{C}$, and $|\alpha|^2 + |\beta|^2 = 1$. According to Eqs. (18)-(24), after an interaction time $t = \pi/\Omega$, the final system state becomes

$$|\Psi_F\rangle = |\downarrow_1\rangle\,(\alpha\,|\downarrow_2\rangle + \beta\,|\uparrow_2\rangle)\,|0\rangle_{\rm NV}\,. \tag{32}$$

The quantum information in nuclear spin 1 is transferred to nuclear spin 2.

To gain insight into the origin of this QST, we begin to consider a subset of Hilbert subspaces of the system (see Fig. 5). Dipole-dipole interaction causes a splitting of the system energy, with the corresponding energy eigenvalues

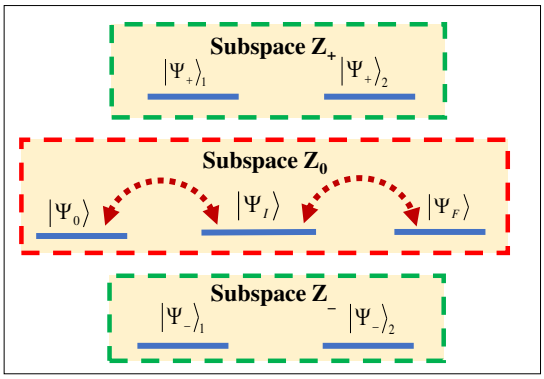

FIG. 5: (Color online) Schematic Hilbert subspaces for QST. Due to the dipole-dipole interaction, the system energy is split into three energy levels. The eigenvalues are $\lambda = 0$, $\lambda_+ = \sqrt{2}g$ and $\lambda_- = -\sqrt{2}g$, with the corresponding Hilbert subspaces Z_0, Z_+ and Z_-. In the dark subspace Z_0, an intermediate state $|\Psi_I\rangle$ couples with $|\Psi_0\rangle$ and $|\Psi_F\rangle$, via the driving by the mechanical wave (denoted by dot lines).

$\lambda = 0$, $\lambda_+ = \sqrt{2}g$, and $\lambda_- = -\sqrt{2}g$, respectively. Then the total Hilbert space is split into three corresponding invariant subspaces

$$\begin{aligned} Z_0 &= \{|\Psi_0\rangle\,, |\Psi_F\rangle\,, |\Psi_I\rangle\}, \\ Z_+ &= \{|\Psi_+\rangle_1\,, |\Psi_+\rangle_2\}, \\ Z_- &= \{|\Psi_-\rangle_1\,, |\Psi_-\rangle_2\}, \end{aligned} \tag{33}$$

where

$$\begin{aligned} |\Psi_I\rangle =& \frac{1}{2}(|\downarrow_1\rangle\,|\uparrow_2\rangle - |\uparrow_1\rangle\,|\downarrow_2\rangle)(|\downarrow\rangle_{\rm NV} + |\uparrow\rangle_{\rm NV}), \\ |\Psi_\pm\rangle_1 =& \frac{1}{2}\left[(|\uparrow_1\rangle\,|\downarrow_2\rangle + |\downarrow_1\rangle\,|\uparrow_2\rangle)\,|\downarrow\rangle_{\rm NV} \pm \sqrt{2}\,|\downarrow_1\rangle\,|\downarrow_2\rangle\,|\uparrow\rangle_{\rm NV}\right], \\ |\Psi_\pm\rangle_2 =& \frac{1}{2}\left[(|\uparrow_1\rangle\,|\downarrow_2\rangle + |\downarrow_1\rangle\,|\uparrow_2\rangle)\,|\uparrow\rangle_{\rm NV} \pm \sqrt{2}\,|\uparrow_1\rangle\,|\uparrow_2\rangle\,|\downarrow\rangle_{\rm NV}\right]. \end{aligned} \tag{34}$$

Large splitting of energy levels results in the difficulty of the transitions between different energy levels. However,

the states belong to the same energy level interact with each other easily. If the initial state lies in the invariant subspace Z_0, the survival probability in Z_0 remains unity. A field drives the state transition from $|\Psi_0\rangle$ to $|\Psi_I\rangle$, and then from $|\Psi_I\rangle$ to $|\Psi_F\rangle$, as shown in Fig. 5. Mediated by the NV center, the quantum state is transferred between two distant nuclear spins,

$$\begin{aligned}&(\alpha|\downarrow_1\rangle+\beta|\uparrow_1\rangle)|\downarrow_2\rangle|0\rangle_{\rm NV}\\ \rightarrow&(|\downarrow_1\rangle|\uparrow_2\rangle-|\uparrow_1\rangle|\downarrow_2\rangle)(\alpha|\downarrow\rangle_{\rm NV}+\beta|\uparrow\rangle_{\rm NV})\\ \rightarrow&|\downarrow_1\rangle(\alpha|\downarrow_2\rangle+\beta|\uparrow_2\rangle)|0\rangle_{\rm NV}.\end{aligned}\tag{35}$$

This process can be generalized to perform QST between any pair of multiple nuclear spins.

Now, we investigate the effect of systematic errors, which are caused by fixed fluctuations on the system parameters. For example, the fluctuation of driving-field Rabi frequency Ω can be assumed as a fixed value $\delta\Omega=\Omega^{'}-\Omega$ with $\Omega^{'}$ being the real value in experiment. $H_{\rm DD}$ in Eq. (12) describes dipole-dipole interaction between the NV center spin and nuclear spins. A small uncertainty or variation in the separation r leads to a corresponding change in g. A small fluctuation of the interaction time t also affects QST. Thus, we consider three factors during the process of QST. Figure 6 shows that small fluctuations of g, Ω and t have little impact on the fidelity of QST, on condition that $\Omega\ll g$. Even a large fluctuation ($\delta g/g=0.1$, $\delta t/t=0.1$), the fidelity remains high (≥ 0.98). The results of numerical simulation in fact demonstrate that QST between a nuclear-spin pair is robust against variations and uncertainty in the distance between the NV center and nuclear spins.

Considering the hybrid quantum devices based on NV centers in diamond, the dominant decoherence mechanism is photon emission via exciton decays of the NV center. In our scheme, according to quantum Zeno dynamics, weakly driving field keeps the NV center staying in its ground state. It is helpful to improve the fidelity of entangling gates, as the same effect of reinitializing the NV center to $|0\rangle$ [55]. If system is initially in the state $|0\rangle$, the survival probability reads

$$P_0(t)=\left[\frac{g^2+\Omega^2\cos(\sqrt{g^2+\Omega^2}t)}{g^2+\Omega^2}\right]^2.\tag{36}$$

As shown in Fig. 7, in regime $g\gg\Omega$, the survival probability in ground state $|0\rangle$ is about 1. The probability in excited state is so small that the photon emission is suppressed.

Now, numerical simulations are used to show influences of spontaneous decay and off-resonant coupling. As shown in Fig. 8, when the spontaneous decay rate of NV center $\gamma_{\rm NV}/g\geq 0.01$, with the scaled off-resonant strength $\Delta/g=0.01$, the fidelity $F\geq 0.94$. However, the fidelity $F\geq 0.97$, when the spontaneous decay rate of nuclear spin $\gamma_{\rm N}/g\geq 0.01$. Thus, under the quantum Zeno condition, small off-resonant couplings and small decay rate of the NV center have little impact on the fidelity of QST.

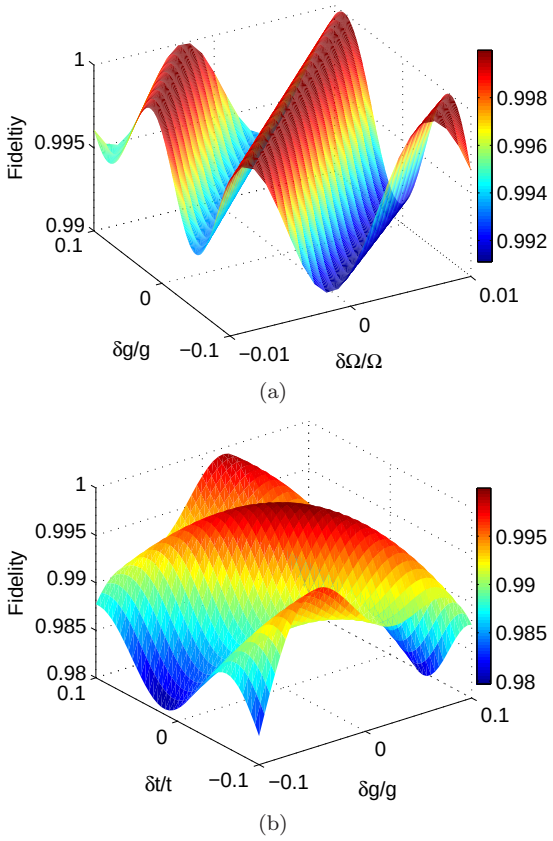

FIG. 6: (Color online) The fluctuation of the interaction time, the coupling strength, and the Rabi frequency of driving field influence the fidelity of QST, considering no spontaneous decay, for the original $g\sim 2\pi\times 2$ MHz and $\Omega\sim 2\pi\times 210$ kHz. (a) The fidelity of QST versus $\delta g/g$ and $\delta\Omega/\Omega$. (b) The fidelity of QST versus $\delta g/g$ and $\delta t/t$ with the original interaction time $T=\pi/\Omega$.

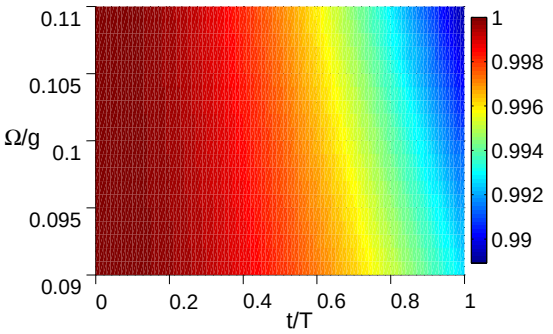

FIG. 7: (Color online) The survival probability in ground state $|0\rangle$ of NV center $P_0(t)$ versus the scaled time t/T and Ω/g, with $g\sim 2\pi\times 2$MHz and the interaction time $T=\pi/\Omega$.

V. DISCUSSION

In this section, we explain the experimental realization of our model and present further applications. We first discuss how to prepare and manipulate the sys-

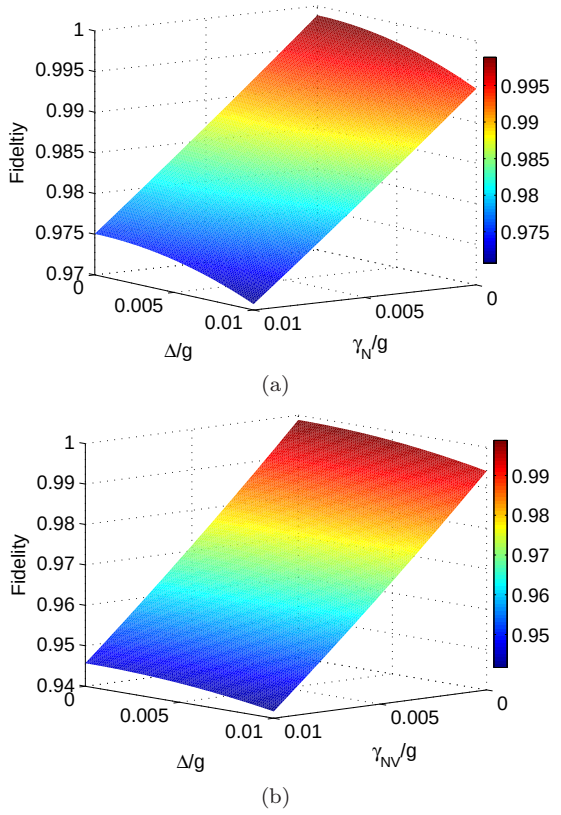

FIG. 8: (Color online) The off-resonant coupling and the spontaneous decay of NV center and nuclear spin influence the fidelity of QST with $g \sim 2\pi \times 2$ MHz and $\Omega \sim 2\pi \times 210$ kHz, for $t = \pi/\Omega$. (a) The fidelity of QST versus $\gamma_{\rm N}/g$ and Δ/g. (b) The fidelity of QST versus $\gamma_{\rm NV}/g$ and Δ/g.

tem spin states. Linearly polarized optical excitation preferentially pumps the NV center spin into ground state $|m_s = 0\rangle_{\rm NV}$. The laser is then turned off and a magnetic adiabatic passage through the $|m_s = 0\rangle_{\rm NV} \rightarrow |m_s = +1\rangle_{\rm NV}$ resonance robustly transfers the initialized spin population into the state $|m_s = +1\rangle_{\rm NV}$ [17], which is the initial NV center spin state we need. Then, let magnetic-dipole coupling and mechanically driving take effect. A stress wave is turned on at a frequency $\omega_{\rm HBAR}$ corresponding to a resonance of the HBAR. The mechanical spin resonance $|m_s = +1\rangle_{\rm NV} \rightarrow |m_s = -1\rangle_{\rm NV}$ spin transition can be detected via optical pulses.

From the simulations above we can see that fidelity of the scheme is spoiled by dephasing. Therefore, implementing this proposal with high fidelity requires that the dephasing rate $\gamma_{\rm NV}, \gamma_{\rm N} \ll g$. The relaxation time T_1 of an NV center can be achieved the order of seconds at low temperature around 4 K [46]. The decoherence time T_2 can be prolonged to 15 μs using a continuous dynamical decoupling of a NV center spin with a mechanical resonator [56]. In addition, in high purity diamond, T_2 of a single NV center is longer than 600 μs at room temperature [57]. Nuclear spins have long relaxation and coherence time in comparison with those of electron spins in diamond. The relaxation time of single nuclear spin $T_1 = (75 \pm 20)$ μs at room temperature [41]. The operating time required of entangling gates or QST is $t = \pi/\Omega \approx 2.5$ μs, which is far less than T_1 and T_2 of the NV center (or nuclear spins). Therefore reasonable values of fidelity in our scheme can be anticipated.

Normally, driving NV electron spins independently of the nuclear spins is not easy. In our scheme, mechanical spin control of NV center and magnetic dipolar coupling of nuclear-NV spins is a good alternative. However, there are also some challenges in experimental realization of our model. It is challenging to individually address one of the nuclear spins without affecting the other, no matter whether two nuclear spins have similar couplings to the NV center or not.

Our scheme can be extended to multi-qubit systems. A NV center spin is placed at the center of a polygon geometry with each vertex occupied by a nuclear spin. Based on our scheme, any two nuclear spins indirectly interact. Considered the polygon geometry a basic unit, many-body location can be achieved mediated by the interactions between distant NV centers [58]. Furthermore, it may be used for simulating spin models with topological order [59].

This scheme also can be applied in biological probe. Nuclear spins in a single molecule were studied to learn structural information in chemical and biological processes [60]. Through dipole coupling to nuclear spins, a NV center can effectively act as a dipole "antenna", detecting spins at different spatial locations. For example, NV centers can be used to detect the charge recombination rate in a radical pair reaction [61].

VI. CONCLUSIONS

In summary, based on quantum Zeno effect and dipole-dipole coupling, we present a protocol for the generation of entangling gates and quantum-state transfer between two separated nuclear spins mediated by a NV center in diamond. The system coherently evolves within the quantum Zeno dark subspaces. The results of numerical simulations show that our protocol is robust against the fluctuations of external fields, and the uncertainty of the distance between the NV center and nuclear spins.

VII. ACKNOWLEDGMENTS

The authors acknowledge J. P. Hadden and H.-Z. Wu for helpful discussions and suggestions. This work is supported by the National Natural Science Foundation of China under Grant No. 11405031, the National Natural Science Foundation of Fujian Province under Grant No. 2018J0106.

[1] B. E. Kane, Nature (London) **393**, 133 (1998).
[2] A. Lvovsky, B. C. Sanders, and W. Tittel, Nat. Photon. **3**, 706 (2009).
[3] J. J. L. Morton, A. M. Tyryshkin, R. M. Brown, S. Shankar, B. W. Lovett, A. Ardavan, T. Schenkel, E. E. Haller, J. W. Ager, and S. A. Lyon, Nature (London) **455**, 1085 (2008).
[4] D. L. Sage, K. Arai, D. R.Glenn, S. J. DeVience, L. M. Pham, L. Rahn Lee, M.D. Lukin, A. Yacoby, A. Komeili, and R. L. Walsworth, Nature (London) **496**, 486 (2013).
[5] J.-M Cai, F. Jelezko, M. B. Plenio, and A. Retzker, New J. Phys., **15**, 013020 (2013).
[6] H. Bernien, B. Hensen, W. Pfaff, G. Koolstra, M. S. Blok, L. Robledo, T. H. Taminiau, M. Markham, D. J. Twitchen, L. Childress, and R. Hanson, Nature (London) **497**, 86 (2013).
[7] P.-B. Li, Z.-L. Xiang, P. Rabl, and F. Nori, Phys. Rev. Lett. **117**, 015502 (2016).
[8] Y. K. Kato R. J. Epstein, F. M. Mendoza, and D. D. Awschalom, Nat. Phys. **1**, 94 (2005).
[9] G. Waldherr, Y. Wang, S. Zaiser, M. Jamali, T. Schulte-Herbrüggen, H. Abe, T. Ohshima, J. Isoya, J.-F. Du, P. Neumann, and J. Wrachtrup, Nature (London) **506**, 204 (2014).
[10] P.-B. Li, Y.-C. Liu, S.-Y. Gao, Z.-L. Xiang, P. Rabl, Y.-F. Xiao, and F.-L. Li, Phys. Rev. Appl. **4**, 044003 (2015).
[11] A. Ajoy, U. Bissbort, M. D. Lukin, R. L. Walsworth, and P. Cappellaro, Phys. Rev. X **5**, 011001 (2015).
[12] Q. Chen, I. Schwarz, and M. B. Plenio, Phys. Rev. Lett. **119**, 010801 (2017).
[13] P. Rabl, S. J. Kolkowitz, F. H. L. Koppens, J. G. E. Harris, P. Zoller, and M. D. Lukin, Nat. Phys. **6**, 602 (2010).
[14] B. D′Urso, M. V. G. Dutt, S. Dhingra, and N. M. Nusran, New J. Phys. **13** 045002 (2011).
[15] K. V. Kepesidis, S. D. Bennett, S. Portolan, M. D. Lukin, and P. Rabl, Phys. Rev. B **88**, 064105 (2013).
[16] D. A. Golter, T. Oo, M. Amezcua, I. Lekavicius, K. A. Stewart, and H. Wang, Phys. Rev. X **6**, 041060 (2016).
[17] E. R. MacQuarrie, T. A. Gosavi, N. R. Jungwirth, S. A. Bhave, and G. D. Fuchs, Phys. Rev. Lett. **111**, 227602 (2013).
[18] B. Misra and E. C. G. Sudarshan, J. Math. Phys. **18**, 756 (1977).
[19] P. Facchi and S. Pascazio, Phys. Rev. Lett. **89**, 080401 (2002).
[20] A. Beige, D. Braun, B. Tregenna, and P. L. Knight, Phys. Rev. Lett. **85**, 1762 (2000).
[21] P. Facchi and S. Pascazio, J. Phys. A **41**, 493001 (2008).
[22] P. Facchi, V. Gorini, G. Marmo, S. Pascazio, and E. C. G. Sudarshan, Phys. Lett. A **275**, 12 (2000).
[23] R. J. Cook, Phys. Scr. **T21**, 49 (1988)
[24] W. M. Itano, D. J. Heinzen, J. J. Bollinger, and D. J. Wineland, Phys. Rev. A **41**, 2295 (1990).
[25] J. M. Raimond, P. Facchi, B. Peaudecerf, S. Pascazio, C. Sayrin, I. Dotsenko, S. Gleyzes, M. Brune, and S. Haroche, Phys. Rev. A **86**, 032120 (2012).
[26] F. Schäfer, I. Herrera, S. Cherukattil, C. Lovecchio, F. S. Cataliotti, F. Caruso, and A. Smerzi, Nat. Commun. **5**, 3194 (2014).
[27] S. Hacohen-Gourgy, L. P. Garcia-Pintos, L.S. Martin, J. Dressel, and I. Siddiqi, Phys. Rev. Lett. **120**, 020505 (2018).
[28] Fei Kong, ChenYong Ju, Pu Huang, Pengfei Wang, Xi Kong, Fazhan Shi, Liang Jiang, and Jiangfeng Du, Phys. Rev. Lett. **115**, 080501 (2015).
[29] M. Saffman, T. G. Walker, and K. Mølmer, Rev. Mod. Phys. **82**, 2313 (2010).
[30] M. D. Lukin, and P. R. Hemmer, Phys. Rev. Lett. **84**, 2818 (2000).
[31] E. Brion, L. H. Pedersen, and K. Mølmer, J. Phys. B **40**, S159 (2007).
[32] H.-Z Wu, Z.-B. Yang, and S.-B. Zheng, Phys. Rev. A **82**, 034307 (2010).
[33] D. Jaksch, J. I. Cirac, P. Zoller, S. L. Rolston, R. Côté, and M. D. Lukin, Phys. Rev. Lett. **85**, 2208 (2000).
[34] S.-L. Su, Y. Gao, E. Liang, and S. Zhang, Phys. Rev. A **95**, 022319 (2017).
[35] X.-Q. Shao, J.-H. Wu, and X.-X. Yi, Phys. Rev. A **95**, 062339 (2017).
[36] J. R. Maze, A. Gali, E. Togan, Y. Chu, A. Trifonov, E. Kaxiras, and M. D. Lukin, New J. Phys. **13**, 025025 (2011).
[37] H.-Z. Wu, X.-R. Huang, C.-S. Hu, Z.-B. Yang, and S.-B. Zheng, Phys. Rev. A **96**, 022321 (2017).
[38] H. Weimer, N. Y. Yao, C. R. Laumann, and M. D. Lukin, Phys. Rev. Lett. **108**,100501 (2012).
[39] A. Bermudez, F. Jelezko, M. B. Plenio, and A. Retzker, Phys. Rev. Lett. **107**, 150503 (2011).
[40] C. Belthangady, N. B. Gill, L. M. Pham, K. Arai, D. Le Sage, P. Cappellaro, and R. L. Walsworth, Phys. Rev. Lett. **110**,157601 (2013).
[41] R. Hanson, F. M. Mendoza, R. J. Epstein, and D. D. Awschalom, Phys. Rev. Lett. **97**,087601 (2006).
[42] F. Jelezko, T. Gaebel, I. Popa, A. Gruber, and J. Wrachtrup, Phys. Rev. Lett. **92**, 076401 (2004).
[43] T. Gaebel, M. Domhan, I. Popa, C. Wittmann, P. Neumann, F. Jelezko, J. R. Rabeau, N. Stavrias, A. D. Greentree, S. Prawer, J. Meijer, J. Twamley, P. R. Hemmer, and J. Wrachtrup, Nat. Phys. **2**, 408 (2006).
[44] R. Hanson, V. V. Dobrovitski, A. E. Feiguin, O. Gywat, and D. D. Awschalom, Science **320**, 352 (2008).
[45] S. Felton, A. M. Edmonds, M. E. Newton, P. M. Martineau, D. Fisher, D. J. Twitchen, and J. M. Baker, Phys. Rev. B **79**, 075203 (2009).
[46] J. Cramer, N. Kalb, M.A. Rol, B. Hensen, M.S. Blok, M. Markham, D. J. Twitchen, R. Hanson, and T. H. Taminiau, Nat. commun. **7**, 11526 (2016).
[47] E. Togan, Y. Chu, A. S. Trifonov, L. Jiang, J. Maze, L. Childress, M. V. G. Dutt, A. S. Sørensen, P. R. Hemmer, A. S. Zibrov, and M. D. Lukin, Nature (London) **466**, 730 (2010).
[48] P. Meystre, *Atom optics* (Springer-Verlag, New York, 2001).
[49] A. Uhlmann, Rep. Math. Phys. **9**, 273 (1976).
[50] Z.-B. Yang, H.-Z. Wu, W.-J. Su, and S.-B. Zheng, Phys. Rev. A 80, 012305 (2009).
[51] L. Banchi, A. Bayat, P. Verrucchi, and S. Bose, Phys. Rev. Lett. **106**, 140501 (2011).
[52] S. Lloyd, Science **261**, 1569 (1993).
[53] D. W. Berry and B. C. Sanders, Phys. Rev. Lett. **90**, 057901 (2003).

[54] S.-B. Zheng and G.-C. Guo, Phys. Rev. Lett. **85**, 2392 (2000).
[55] Q. Chen, I. Schwarz, and M. B. Plenio, Phys. Rev. B **95**, 224105 (2017).
[56] E. R. MacQuarrie, T. A. Gosavi, S. A. Bhave, and G. D. Fuchs, Phys. Rev. B **92**, 224419 (2015).
[57] J. R. Maze, P. L. Stanwix, J. S. Hodges, S. Hong, J. M. Taylor, P. Cappellaro, L. Jiang, M. V. Gurudev Dutt, E. Togan, A. S. Zibrov, A. Yacoby, R. L. Walsworth, and M. D. Lukin, Nature (London) **455**, 644 (2008).
[58] N. Y. Yao, C. R. Laumann, S. Gopalakrishnan, M. Knap, M. Müller, E. A. Demler, and M. D. Lukin, Phys. Rev. Lett. **113**, 243002 (2014).
[59] X.-L. Qi and S.-C. Zhang, Rev. Mod. Phys. **83**, 1057 (2011).
[60] W. E. Moerner and M. Orrit, Science **283**, 1670 (1999).
[61] H.-B Liu, M. B. Plenio, and J.-M. Cai, Phys. Rev. Lett. **118**, 200402 (2017).